Received January 16, 2022, accepted January 23, 2022, date of publication February 4, 2022, date of current version February 14, 2022.
Digital Object Identifier 10.1109/ACCESS.2022.3149135

Multi-Objective Optimization for Optimal Allocation and Coordination of Wind and Solar DGs, BESSs and Capacitors in Presence of Demand Response

HAITHAM A. TAHA, M. H. ALHAM, AND HOSAM K. M. YOUSSEF
Faculty of Engineering, Cairo University, Giza 12613, Egypt
Corresponding author: Haitham A. Taha (haitham.taha.1@gmail.com)

ABSTRACT The renewable energy sources (RES) based distributed generations (DGs) have been proven to be of great technical and economic benefits if optimally allocated in distribution networks. Their proper deployment is usually made in conjunction with demand response (DR) programs and renewables curtailment to match the demand load with the available generated power. Battery energy storage systems (BESSs) and capacitor banks (CBs) are two other tools that can compensate for the shortcomings of the RES. BESSs could complement the renewables generation intermittency and improve the reliability of the system while CBs could indemnify the limited reactive power support of the RES and improve the power quality of the system. Thus, the simultaneous integration of RES-based DGs, DR, BESSs, CBs, and curtailment could have great benefits if optimally planned and coordinated. In this paper, a multi-objective optimization planning model is formulated to determine the optimal locations and capacities of different RES-based DGs, BESSs, and CBs in presence of DR and renewables curtailment to maximize the economic index and the average voltage stability factor, and to minimize the average power losses in distribution networks. The modelling of RES-generated power is considered. The proposed model is implemented and tested on standard IEEE 33-bus radial distribution system, the model is formulated and solved in GAMS environment. Different renewable configurations and test cases are investigated. The obtained results validate the effectiveness of the simultaneous integration of the used tools in optimizing the techno-economic benefits.

INDEX TERMS Multi-objective optimization, renewable energy sources, battery energy storage systems, battery degradation, capacitor banks, demand response, economic index, losses, voltage stability factor, wind, solar, distributed generations.

NOMENCLATURE

t	Time in hours.
i, j	Network buses.
$f_v^t\ (v)$	Weibull distribution of wind speed (v^t) over time t.
c^t, k^t	Scale and shape parameters of Weibull probability distribution function
v^t	Wind speed at time t, m/sec.
$\mu\sigma_w^t, {}_w^t$	Mean and standard deviation of wind speed.
Γ	Gamma function.
P_r^{WDG}	Rated power of wind turbine, kW.
$v_{ci}/v_{co}/v_r$	Cut-in/cut-out/rated speed of wind turbine, m/sec.
$P^{WDG}(v^t)$	Generated wind power at wind speed $\left(v^t\right)$, kW.
$f_s^t\ (S)$	Beta distribution for solar irradiance (S^t) over time t.
α^t, β^t	Shape parameters of Beta probability distribution function.
μ_s^t, σ_s^t	Mean and standard deviation of solar irradiance over time t.
$P^{SDG}(S^t)$	Generated solar power at solar irradiance $\left(S^t\right)$, kW.
η	Efficiency of solar photovoltaic panels.

The associate editor coordinating the review of this manuscript and approving it for publication was Lei Chen.

A_{PV} Area of the installed solar photovoltaic panels, m^2.
S^t Solar irradiance at time t, kW/ m^2.
T_{PV} PV panels cell temperature, °C.
EI Economic index.
ACS Annual cost saving
$ADRC$ Annual demand response compensation.
ACP^{DG} Annual capital cost of renewable DGs.
$AOMC^{DG}$ Annual operation and maintenance cost of renewable DGs.
ACP^{BESS} Annual capital cost of BESSs.
ACP^{CB} Annual capital cost of CBs.
P_t^{GO} Original active power supplied by the grid on substation bus at time t in the base case with no DGs, DR, BESSs, CBs and curtailment, kW.
P_t^G Active power supplied by the grid on substation bus at time t after integration of DGs, DR, BESSs, CBs and curtailment, kW.
CPV^y Current present value factor.
C_{hr} Purchased electricity rate per kWh.
N_y Life time of the installations, years.
IF Annual inflation rate.
IR^* Annual nominal interest rate.
N_{day} Number of days per year.
C_{hr}^{DR} DR compensation rate per kWh.
t_{DR} Peak demand hours during which DR compensation is paid, Hours.
IC_i^{WDG}/IC_i^{SDG} Installation cost of renewable wind/solar DG installed at bus i.
CRF^{WDG} Capital recovery factor of renewable wind DGs.
CRF^{SDG} Capital recovery factor of renewable solar DGs.
IC_i^{BESS} Installation cost of BESS installed at bus i.
IC_i^{CB} Installation cost of CB installed at bus i.
CRF^{BESS} Capital recovery factor of BESSs.
CRF^{CB} Capital recovery factor of CBs.
LP Life period of installed component, years.
IR Annual real interest rate.
OMC_i^{WDG} Operation and maintenance cost of renewable wind DG installed at bus i.
OMC_i^{SDG} Operation and maintenance cost of renewable solar DG installed at bus i.
OMC_i^{BESS} Operation and maintenance cost of BESS installed at bus i.
N_{yWDG}/N_{ySDG} Life time of wind/solar DGs, years.
N_{yBESS} Life time of BESSs, years.
N_{yCB} Life time of CBs, years.
$DegC^{BESS}$ Degradation cost of BESS per kWh of the discharged energy.
EC^{BESS} Installation cost of BESS per kWh.
$DegC^{BESS-REF}$ Degradation cost of reference BESS per kWh of the discharged energy.
$EC^{BESS-REF}$ Installation cost of reference BESS per kWh.
P_{LOSS}^{AV} Daily average active power losses, kW.
VSF^{AV} Daily average voltage stability factor.
VSF_t Voltage stability factor at time t.
$\varepsilon 1, \varepsilon 2$ Epsilon parameters.
$S_{ij,t}/P_{ij,t}/Q_{ij,t}$ Apparent/active/reactive power flow between buses i, j at time t, kVA/kW/kVAr.
$V_{i,t}/\delta_{i,t}$ Bus (i) voltage magnitude/voltage angle at time t.
$V_{j,t}/\delta_{j,t}$ Bus (j) voltage magnitude/voltage angle at time t.
Z_{ij}/O_{ij} Line ij impedance/ impedance angle.
$P_{i,t}^{WDG}/Q_{i,t}^{WDG}$ Active/reactive power generation by wind DGs on bus i at time t, kW/kVAr.
$P_{i,t}^{SDG}/Q_{i,t}^{SDG}$ Active/reactive power generation by solar DGs on bus i at time t, kW/kVAr.
$P_{i,t}^G/Q_{i,t}^G$ Active/reactive power injected by grid on bus i at time t, kW/kVAr.
$P_{i,t}^D/Q_{i,t}^D$ Active/reactive demand load on bus i at time t, kW/kVAr.
$P_{i,t}^{DO}/Q_{i,t}^{DO}$ Originally expected active/reactive demand load on bus i at time t (without DR), kW/kVAr.
$P_{i,t}^{WDG-CU}$ Curtailed wind power on bus i at time t, kW.
$P_{i,t}^{SDG-CU}$ Curtailed solar power on bus i at time t, kW.
$P_{i,t}^{BESS-CH}$ Charging power of BESS on bus i at time t, kW.
$P_{i,t}^{BESS-DI}$ Discharging power of BESS on bus i at time t, kW.
$Q_{i,t}^{CAP}$ Reactive power of capacitor bank on bus i at time t, kVAr.
$\alpha_i^{DRmin}, \alpha_i^{DRmax}$ Lower and upper limits of DR at bus i.
Δ_t Duration of time interval t, hour.
W_icap Installed wind DG capacity at bus i, kW.
S_icap Installed solar DG capacity at bus i, kW.
W_t/S_t Wind/solar generation pattern at time t.
$\lambda_i^{WDG}/\lambda_i^{SDG}$ Maximum allowed power curtailment percentage of wind/solar DG at bus i.
$PF_{i,t}^{WDG}/PF_{i,t}^{SDG}$ Power factor of wind/solar DG on bus i at time t.
$Q_{i,t}^{WDGmin}$ Lower limit of wind DG reactive power on bus i at time t, kVAr.
$Q_{i,t}^{WDGmax}$ Upper limit of wind DG reactive power on bus i at time t, kVAr.

$Q_{i,t}^{SDGmin}$	Lower limit of solar DG reactive power on bus i at time t, kVAr.
$Q_{i,t}^{SDGmax}$	Upper limit of solar DG reactive power on bus i at time t, kVAr.
V_i^{min}, V_i^{max}	Lower and upper limits of voltage at bus i, pu.
$SOC_{i,t}$	State of charge of BESS on bus i at time t, kWh.
$SOC_{i,t-1}$	State of charge of BESS on bus i at time $t-1$, kWh.
SOC_i^{min}	Lower limit of SOC of BESS at bus i, kWh.
SOC_i^{max}	Upper limit of SOC of BESS at bus i, kWh.
$\eta^{BESS-CH}$	BESS charging efficiency.
$\eta^{BESS-DI}$	BESS discharging efficiency.
$P_i^{BESS-CHmin}$	Lower limit of charging power of BESS at bus i, kW.
$P_i^{BESS-CHmax}$	Upper limit of charging power of BESS at bus i, kW.
$P_i^{BESS-DImin}$	Lower limit of discharging power of BESS at bus i, kW.
$P_i^{BESS-DImax}$	Upper limit of discharging power of BESS at bus i, kW.
Q_i^{CAPmin}	Lower limit of capacitor bank rating at bus i, kVAr.
Q_i^{CAPmax}	Upper limit of capacitor bank rating at bus i, kVAr.

I. INTRODUCTION

The utilization of renewable energy sources (RES) is steadily increasing to meet the rising electricity demand worldwide. This increase is mainly driven by the environmental benefits the RES afford over the traditional power plants including reduction of carbon emissions and global warming, and economic benefits supported by the RES energy generation cost fall and the creation of million jobs. The wind and solar RES are currently having the highest contribution in the renewable energy mix globally and are expected to continue their tremendous growth to take the lead in the global energy mix over the conventional power plants [1]. The penetration levels of wind and solar RES have some power quality limitations owing to intermittency and uncertainty, however the utilities have ambitious goals of penetration levels due to the aforementioned environmental and economic advantages [2].

One of the distinguishing features of the RES-based DGs is that they have small sizes and ratings compared to centralized traditional plants which allow them to be integrated in distribution networks, they may have great benefits if optimally allocated. The optimal allocation of the RES-based DGs in the distribution networks has several optimization algorithms including classical and artificial intelligence approaches that have been reviewed and compared in [3]–[6], the DGs optimal allocation may also have different objectives. A biogeography-based optimization was proposed in [7] for optimal location and sizing of solar photovoltaic DG units to reduce the power losses while maintaining the voltage profile and voltage harmonic distortion within the limits. In [8], a Weibull distribution-based time-coupled probabilistic generation model was presented for the optimal placement and sizing of wind DG with time-varying voltage-dependent loads to minimize the average multi-objective index which combines power losses, voltage drop, and voltage stability indices.

Authors in [9], [10] proposed approaches for the optimal allocation of RES and reconfiguration in distribution networks to minimize the cost of power losses, improve reliability, and enhance the voltage profile.

The proper deployment of RES-based DGs is usually made in conjunction with demand response programs that help to match the demand load with the available generated power.

The DR programs are developed to motivate the change in energy consumption of customers, in response to changes in the price of electricity over time, or to give incentive payments designed to induce lower electricity use at times of high market prices or when grid reliability is jeopardized. The DR has been used in many papers in coordination with RES for the optimal operation of distribution systems [11]–[16].

Renewables curtailment is another tool that has been used in [16], [17] to support the integration of RES.

BESSs and CBs are two other tools that have been numerously used in the literature to offset the shortfalls of the RES. BESSs could manage intermittency and mismatching between renewables generation and demand load, and improve the reliability of the system while CBs could reimburse the limited reactive power support of the RES-based DGs and improve the power quality of the system.

Refs. [18]–[23] discussed the utilization of BESSs in coordination with RES. In [18], a stochastic mathematical model was introduced for the optimal allocation of energy storage units in active distribution networks to reduce wind power spillage and load curtailment while managing congestion and voltages deviation. A technique was proposed in [19] for power system planners and operators to select the power and energy capacity of BESS for mitigating the effects of intermittent wind speeds on reliability and economics. Authors in [20] developed a two-stage planning model for the optimal allocation of the distributed wind turbine, shared BESS, and the optimal dispatch of the individual virtual energy storage system in a smart grid. A multi-objective approach was proposed in [21] for the optimal allocation of centralized wind farm and storage system in distribution network considering technical, environmental, and financial control schemes for the network improvement. In [22], a planning-operation decomposition methodology was introduced for the optimal location, selection, and operation of BESSs and renewable DGs in medium-low voltage distribution systems to minimize the total purchase cost of energy from the distribution substation. A two-stage multi-objective approach was implemented in [23] considering distributed and centralized

RES-based generation units with BESS for maximizing the technical, environmental, and economic benefits including power loss reduction, voltage profile enhancement, voltage stability conditions improvement, emissions reduction, and annual operational cost drop.

The integration between RES and capacitors was discussed in [24]–[27] under various conditions and considering different objectives. A multi-objective planning model was presented in [24] to determine the location and the required installation capacity of multiple PV array, wind turbine, and capacitor units in an electric power distribution network under heavy load growth situation considering possible trade-offs between technical, economic, and environmental objectives. Authors in [25] investigated multi-objective optimal planning of wind and solar DGs, and CBs considering different sources of uncertainty including plug-in electric vehicles. A water cycle algorithm was proposed in [26] for optimal placement and sizing of DGs and CBs to achieve technical, economic, and environmental benefits through different objective functions including minimizing power losses, voltage deviation, total electrical energy cost, and total emissions produced by generation sources, and improving the voltage stability index. Authors in [27] proposed an optimal integration of renewable wind and solar DGs along with biomass and capacitor banks to optimize distribution network parameters.

According to the literature review, it is obvious that the RES-based DGs integration with each of BESSs, CBs, DR, and curtailment tools may offer various benefits if optimally planned and coordinated. The simultaneous integration and coordination of the aforementioned tools with RES have been studied in very few papers. In [28], the optimal coordination of load tap changers, step voltage regulators, switched shunt capacitors, and energy storages with high penetration of PV was performed for minimizing energy loss and improving voltage profile. However, the locations and ratings of PV units and shunt capacitors are assumed to be known. An optimization model was developed in [29] to find optimal dispatches of BESSs in coordination with DR in the presence of wind DGs and shunt capacitors to minimize distribution power loss and grid demand cost. The locations and sizes of BESSs are assumed to be known in [29]. Authors in [30] investigated and applied an optimal multi-configuration and allocation of step-voltage regulators, capacitor banks, energy storage system, and centralized wind-power generation in the distribution network. In [28]–[30] either wind or solar DGs were utilized, also the battery degradation was not considered.

Based on the literature review, the optimal allocation and coordination of renewable wind and solar DGs, BESSs, and CBs for multi-objective technical and economic optimization have not been deeply studied.

In this paper, a planning model is presented for the optimal allocation and coordination of wind and solar DGs, BESSs, and CBs in distribution networks in presence of DR and renewables curtailment, and considering the battery degradation cost. The multi-objective optimization function is formulated to maximize the economic index and the average voltage stability factor, and to minimize the average power losses in distribution networks. The modelling of wind speed and solar irradiance is considered to handle the stochastic nature of wind and solar power. The proposed model is implemented on standard IEEE 33-bus radial distribution system. Multiple configurations and test cases are investigated. The simulation results demonstrate the effectiveness of each of the used tools in fulfilling the multi-objective optimization through maximizing the economic index and the voltage stability factor, and minimizing the power losses in the distribution networks.

The major contributions of this paper are as follows:

1. Simultaneous integration of different RES-based DGs, BESSs, CBs, DR, and curtailment in distribution networks for multi-objective optimization including economic index and average voltage stability factor maximization, and average power losses minimization.
2. Epsilon constraint method is used to form the multi-objective function in which the economic index is optimized subject to average power losses and average voltage stability factor inequality constraints.
3. Modelling of wind speed, solar irradiance, and their associated generated power are considered using scenarios generations through random probability distribution functions in GAMS extrinsic functions and scenarios reduction using fast forward techniques. GAMS environment is also used for mathematical formulation and solution of the optimization problem.
4. Multiple configurations using wind and solar DGs are formulated, in each configuration several cases are studied on IEEE 33-bus radial distribution system.

The rest of this paper is organized as follows: Section II addresses the modelling of renewables generation. Section III introduces the multi-objective optimization problem formulation. Section IV explains the studied cases and discusses the obtained results, while Section V highlights the conclusion.

II. MODELLING OF RENEWABLE POWER GENERATION

Wind and solar power generations are governed by meteorological conditions, namely wind speed and solar irradiance. These conditions should be studied and analyzed for optimum, efficient, and feasible utilization of wind and solar power. Both wind speed and solar irradiance have stochastic nature, the modelling of wind and solar power is addressed in this section:

A. WIND POWER MODELLING

The behavior of wind speed is assumed to follow the Weibull probability distribution function (PDF). Weibull distribution $f_v^t(v)$ for wind speed v^t at time t can be expressed as [24]:

$$f_v^t(v) = \frac{k^t}{c^t}\left(\frac{v^t}{c^t}\right)^{k^t-1}.\exp\left(-\frac{v^t}{c^t}\right)^{k^t} \quad (1)$$

The shape and scale parameters (k^t, c^t) of Weibull PDF can be calculated by:

$$k^t = \left(\frac{\sigma_w^t}{\mu_w^t}\right)^{-1.086}; \quad c^t = \frac{\mu_w^t}{\Gamma\left(1+\left(1/k^t\right)\right)} \quad (2)$$

In this study, the shape and scale parameters of Weibull PDF are taken as 1.4 and 6 m/s, respectively [31].

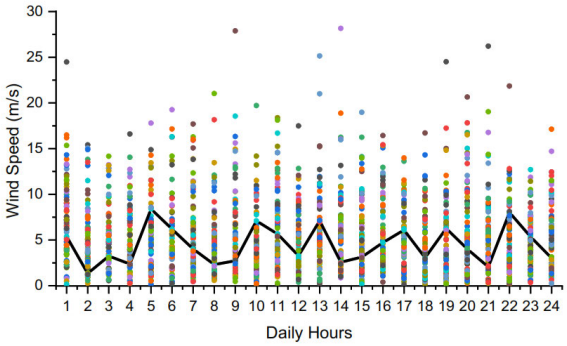

FIGURE 1. Random generated wind speed scenarios following Weibull distribution.

A large number of daily wind speed scenarios are generated using random Weibull function in GAMS built-in extrinsic functions. The generated wind speed scenarios have been reduced using the fast forward selection algorithm. The random generated daily wind speed scenarios are shown in Fig.1 including the most probable scenario which is marked in a black line.

The power of wind DG at wind speed (v^t) is calculated as [30]:

$$P^{WDG}(v^t)=\begin{cases} P_r^{WDG}.\left(\dfrac{v^t-v_{ci}}{v_r-v_{ci}}\right) & for\ v_{ci}\le v^t\le v_r \\ P_r^{WDG} & for\ v_r\le v^t\le v_{co} \\ 0 & for\ v^t\le v_{ci}, v^t\ge v_{co} \end{cases} \tag{3}$$

The per unit wind power pattern for the most probable wind speed scenario is shown in Fig.2.

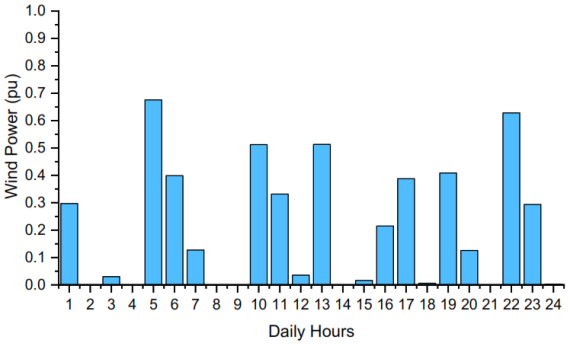

FIGURE 2. Wind power pattern for the most probable wind speed scenario.

The used scenarios generation model in this study doesn't account for the temporal correlation among the wind speed and the associated wind power values of the consecutive time steps. In [32], a generate-rearrange-eliminate algorithm was proposed which reflects the correlation between the wind power output at time t and that of time $t-1$.

The speed parameters of the DG wind turbines are shown in table 1 [24].

TABLE 1. The speed parameters of the DG wind turbines.

Parameter	Value
Cut-in speed (v_{ci})	3 m/s
Rated speed (v_r)	12 m/s
Cut-out speed (v_{co})	25 m/s

B. SOLAR POWER MODELLING

The behavior of solar irradiance is assumed to follow the Beta PDF. Beta distribution $f_s^t(S)$ for solar irradiance S^t over time t is given by [24]:

$$f_s^t(S)=\frac{\Gamma\left(\alpha^t+\beta^t\right)}{\Gamma\left(\alpha^t\right).\Gamma\left(\beta^t\right)}.\left(S^t\right)^{\alpha^t-1}.\left(1-S^t\right)^{\beta^t-1} \tag{4}$$

The shape parameters of Beta PDF can be calculated using the mean (μ_s^t) and standard deviation (σ_s^t) of solar irradiance for corresponding time as follows:

$$\beta^t=\left(1-\mu_s^t\right).\frac{\mu_s^t\left(1+\mu_s^t\right)}{(\sigma_s^t)^2}-1 \tag{5}$$

$$\alpha^t=\frac{\mu_s^t.\beta^t}{\left(1-\mu_s^t\right)} \tag{6}$$

In this study, the shape parameters of Beta PDF are taken as $\alpha=2.57$ and $\beta=1.6$ [31].

A large number of daily solar irradiance scenarios are generated using random Beta function in GAMS built-in extrinsic functions. The generated solar irradiance scenarios

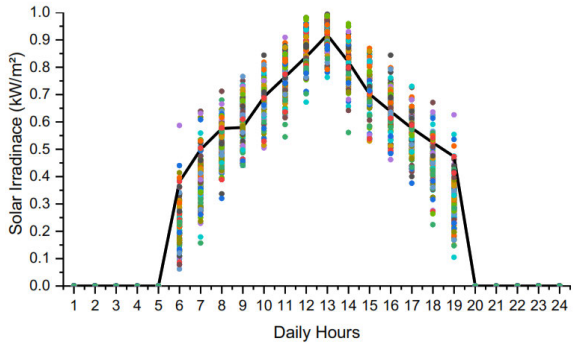

FIGURE 3. Random generated solar irradiance scenarios following Beta distribution.

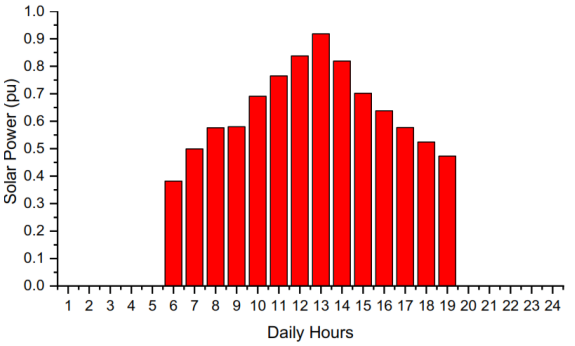

FIGURE 4. Solar power pattern for the most probable solar irradiance scenario.

have been reduced using the fast forward selection algorithm. The random generated daily solar irradiance scenarios are shown in Fig.3 including the most probable scenario which is marked in a black line.

The power of solar DG at solar irradiance (S^t) is calculated as [25].

$$P^{SDG}(S^t) = \eta.A_{PV}.S^t\,(1 - 0.005\,(T_{PV} - 25)) \tag{7}$$

The per unit solar power pattern for the most probable solar irradiance scenario is shown in Fig.4.

III. OPTIMIZATION PROBLEM FORMULATION

The multi-objective optimal allocation and coordination of renewable DGs, battery energy storage systems (BESSs), and capacitor banks (CBs) comprise three main objectives, which are economic index maximization, average power losses minimization, and average voltage stability factor maximization.

A. FIRST OBJECTIVE (OF1): ECONOMIC INDEX MAXIMIZATION

The economic index is a measure of the economic feasibility of certain projects over the planning period. It considers the capital investment cost, operation and maintenance cost of the installed elements. The higher the economic index, the better economic feasibility.

The economic index (EI) can be formulated as in [24] but modified to incorporate the costs of BESSs and DR compensation as follows, (8), as shown at the bottom of the page. The representations of each term in the (EI) formula are described under the following headings.

1) ANNUAL COST SAVING

Due to the integration of renewable DGs, BESSs, and CBs, the annual purchased power from the utility grid shall be reduced. The annual cost saving (ACS) can be calculated as follows:

$$ACS = \frac{\sum_{y=1}^{N_y}\left(\sum_i (P_i^{GO} - P_i^G).\Delta_t.N_{day}\right).CPV^y.C_{hr}}{N_y} \tag{9}$$

The current present value factor (CPV^y) converts the future cost into an equivalent present value. It can be calculated as:

$$CPV^y = \left(\frac{1+IF}{1+IR^*}\right)^y \tag{10}$$

2) ANNUAL DEMAND RESPONSE COMPENSATION

The DR programs provide incentive payments to customers who agree to reduce their energy demand during the peak demand hours.

The annual demand response compensation ($ADRC$) paid to customers can be calculated as:

$$ADRC = \frac{\sum_{y=1}^{N_y}\left(\sum_{i,t_{DR}} (P_{i,t}^{DO} - P_{i,t}^{D}).\Delta_t.N_{day}\right).CPV^y.C_{hr}^{DR}}{N_y} \tag{11}$$

3) ANNUAL CAPITAL COST OF RENEWABLE DG, BESS, AND CB

The annual capital cost of renewable DGs $\left(ACP^{DG}\right)$ can be calculated by:

$$ACP^{DG} = \sum\nolimits_i IC_i^{WDG}.CRF^{WDG} + \sum\nolimits_i IC_i^{SDG}.CRF^{SDG} \tag{12}$$

Similarly, the annual capital cost of BESSs and CBs can be calculated as shown in (13) and (14), respectively.

$$ACP^{BESS} = \sum\nolimits_i IC_i^{BESS}.CRF^{BESS} \tag{13}$$

$$IC_i^{BESS} = ACP^{CB} = \sum\nolimits_i IC_i^{CB}.CRF^{CB} \tag{14}$$

The capital recovery factor (CRF) represents the ratio of a constant annuity for a given length of time to the present value of receiving that annuity. The CRF can be calculated as follows:

$$CRF = \frac{IR.(1+IR)^{LP}}{(1+IR)^{LP} - 1} \tag{15}$$

The annual real interest rate (IR) can be calculated as follows:

$$IR = \frac{(IR^* - IF)}{(1+IF)} \tag{16}$$

4) ANNUAL OPERATION AND MAINTENANCE COST OF RENEWABLE DG AND BESS

The annual operation and maintenance cost of renewable DGs ($AOMC^{DG}$) can be calculated as:

$$AOMC^{DG} = \frac{\sum_{y=1}^{N_{yWDG}} (\sum_i OMC_i^{WDG}).CPV^y}{N_{yWDG}} + \frac{\sum_{y=1}^{N_{ySDG}} (\sum_i OMC_i^{SDG}).CPV^y}{N_{ySDG}} \tag{17}$$

Similarly, the annual operation and maintenance cost of BESSs ($AOMC^{BESS}$) can be calculated as:

$$AOMC^{BESS} = \frac{\sum_{y=1}^{N_{yBESS}} (\sum_i OMC_i^{BESS}).CPV^y}{N_{yBESS}} \tag{18}$$

$$OF1 = EI = \frac{ACS + ADRC}{ACP^{DG} + AOMC^{DG} + ACP^{BESS} + AOMC^{BESS} + ADegC^{BESS} + ACP^{CB}} \tag{8}$$

5) ANNUAL DEGRADATION COST OF BESS

The BESS capability to store energy decreases over time resulting in a capacity fade, power fade, or both. This is as a result of complex electrochemical and mechanical processes inside the battery that can take place simultaneously [33]. In this study, the BESS degradation is considered as a cost per kWh of discharged energy [34].

The degradation cost of BESS per kWh of the discharged energy ($DegC^{BESS}$) can be presented as a function of the BESS installation cost per kWh (EC^{BESS}), the degradation cost can be estimated in equation (19) reference to a BESS of known installation and degradation costs, as suggested in [34].

$$DegC^{BESS} = EC^{BESS} \cdot \frac{DegC^{BESS-REF}}{EC^{BESS-REF}} \tag{19}$$

The annual degradation cost of BESS ($ADegC^{BESS}$) can be calculated as, (20), shown at the bottom of the page.

B. SECOND OBJECTIVE (OF2): POWER LOSSES MINIMIZATION

The integration of renewable DGs, BESSs, and CBs affects the load flow of the power distribution networks and accordingly the power losses. The daily average active power losses (P^{AV}_{LOSS}) can be calculated as:

$$OF2 = P^{AV}_{LOSS} = \frac{\sum_{t=1}^{24} \sum_{i,j}^{P_{ij,t}}}{24} \tag{21}$$

C. THIRD OBJECTIVE (OF3): VOLTAGE STABILITY FACTOR MAXIMIZATION

The voltage stability factor is a widely used tool to measure the proximity of network buses towards the voltage collapse point. The daily average voltage stability factor (VSF^{AV}) can be calculated as:

$$OF3 = VSF^{AV} = \frac{\sum_{t=1}^{24} VSF_t}{24} \tag{22}$$

D. MULTI-OBJECTIVE FUNCTION OPTIMIZATION

The multi-objective function (MOF) consists of three objective functions which should be optimized simultaneously.

$$MOF = (OF1, OF2, OF3) \tag{23}$$

In order to optimize several conflicting objective functions, various methods have been proposed in the literature such as the weighted sum method, ε-constraint method, and goal programming method. In this paper, the ε-constraint method is used to solve the proposed multi-objective optimization model. In this method, one of the objective functions is optimized while the other objectives are considered as inequality constraints, the constraints vary by adjusting the value of ε parameters.

In the proposed model, $OF1$ is optimized, while $OF2$ and $OF3$ are considered as inequality constraints as expressed in (24) to (27).

$$MOF = Maximize\ OF1 \tag{24}$$

$$Subject\ to: \quad OF2 \le \varepsilon 1 \tag{25}$$

$$OF3 \ge \varepsilon 2 \tag{26}$$

$$Other\ technical\ constraints\ as\ addressed\ in\ (E) \tag{27}$$

The epsilon parameters $\varepsilon 1$ and/or $\varepsilon 2$ vary at each iteration, and the multi-objective function is solved.

E. TECHNICAL CONSTRAINTS

The multi-objective function is subject to the following operational and technical constraints:

1) LOAD BALANCE EQUATIONS

The active and reactive power flow equations between buses i and j at time t are expressed in (28) and (29), respectively.

$$\begin{aligned} P_{ij,t} &= Real\left\{S_{ij,t}\right\} \\ &= \frac{V^2_{i,t}}{Z_{ij}} Cos(O_{ij}) - \frac{V_{i,t}.V_{j,t}}{Z_{ij}} Cos(\delta_{i,t} - \delta_{j,t} + O_{ij}) \end{aligned} \tag{28}$$

$$\begin{aligned} Q_{ij,t} &= Img.\left\{S_{ij,t}\right\} \\ &= \frac{V^2_{i,t}}{Z_{ij}} Sin(O_{ij}) - \frac{V_{i,t}.V_{j,t}}{Z_{ij}} Sin(\delta_{i,t} - \delta_{j,t} + O_{ij}) - \frac{bV^2_{i,t}}{2} \end{aligned} \tag{29}$$

The general nodal active and reactive power balance at bus i and time t are expressed in (30) and (31), respectively.

$$\begin{aligned} &P^{WDG}_{i,t} + P^{SDG}_{i,t} + P^{G}_{i,t} - P^{BESS-CH}_{i,t} + P^{BESS-DI}_{i,t} - P^{D}_{i,t} \\ &\quad - P^{WDG-CU}_{i,t} - P^{SDG-CU}_{i,t} = \sum\nolimits_j P_{ij,t} \end{aligned} \tag{30}$$

$$Q^{WDG}_{i,t} + Q^{SDG}_{i,t} + Q^{G}_{i,t} + Q^{CAP}_{i,t} - Q^{D}_{i,t} = \sum\nolimits_j^{Q_{ij,t}} \tag{31}$$

2) DEMAND RESPONSE EQUATIONS

The constraints expressed in (32) and (33) represent the DR limits on bus i at time t.

$$P^{DO}_{i,t}\left(1 - \alpha^{DRmin}_i\right) \le P^{D}_{i,t} \le P^{DO}_{i,t}\left(1 + \alpha^{DRmax}_i\right) \tag{32}$$

$$Q^{DO}_{i,t}\left(1 - \alpha^{DRmin}_i\right) \le Q^{D}_{i,t} \le Q^{DO}_{i,t}\left(1 + \alpha^{DRmax}_i\right) \tag{33}$$

It is assumed that the DR is in the form of load shifting, the daily energy of each bus should be maintained the same, and

$$ADegC^{BESS} = \frac{\sum_{y=1}^{N_{yBESS}} \left(\sum_{i,t} P^{BESS-DI}_{i,t} . \Delta_t . N_{day} / \eta^{BESS-DI}\right) . CPV^y . DegC^{BESS}}{N_{yBESS}} \tag{20}$$

hence the following constraint should be fulfilled:

$$\sum_t (P^D_{i,t}.\Delta_t) = \sum_t (P^{DO}_{i,t}.\Delta_t) \tag{34}$$

3) RENEWABLE POWER GENERATION PATTERNS

The wind power generation follows the generated wind pattern (W_t).

$$P^{WDG}_{i,t} = W_t.W_i cap \tag{35}$$

Considering the following constraints:

$$P^{WDG-CU}_{i,t} \le \lambda^{WDG}_i.W_i cap \tag{36}$$
$$P^{WDG-CU}_{i,t} \le P^{WDG}_{i,t} \tag{37}$$
$$Q^{WDGmin}_{i,t} \le Q^{WDGW}_{i,t} \le Q^{WDGmax}_{i,t} \tag{38}$$
$$Q^{WDG}_{i,t} = P^{WDG}_{i,t} \tan\left(\arccos\left(PF^{WDG}_{i,t}\right)\right) \tag{39}$$

Similarly, solar power generation follows the generated solar pattern (S_t).

$$P^{SDG}_{i,t} = S_t.S_i cap \tag{40}$$

Considering the following constraints:

$$P^{SDG-CU}_{i,t} \le \lambda^{SDG}_i.S_i cap \tag{41}$$
$$P^{SDG-CU}_{i,t} \le P^{SDG}_{i,t} \tag{42}$$
$$Q^{SDGmin}_{i,t} \le Q^{SDG}_{i,t} \le Q^{SDGmax}_{i,t} \tag{43}$$
$$Q^{SDG}_{i,t} = P^{SDG}_{i,t} \tan\left(\arccos(PF^{SDG}_{i,t})\right) \tag{44}$$

4) VOLTAGE LIMITS

Equation (45) represents the minimum and maximum voltage limits on bus i at time t.

$$V^{min}_i \le V_{i,t} \le V^{max}_i \tag{45}$$

5) BATTERY ENERGY STORAGE SYSTEM

Equation (46) shows the state of charge of BESS on bus i at time $t(SOC_{i,t})$ as a function of battery previous state of charge at time $t-1(SOC_{i,t-1})$, battery charging power, and battery discharging power.

$$SOC_{i,t} = SOC_{i,t-1} + \left(P^{BESS-CH}_{i,t}.\eta^{BESS-CH} - P^{BESS-DI}_{i,t}/\eta^{BESS-DI}\right) \cdot \Delta_t \tag{46}$$

Equations (47), (48), and (49) represent the minimum and maximum limits of charging power, discharging power, and state of charge of BESS on bus i at time t, respectively.

$$P^{BESS-CHmin}_i \le P^{BESS-CH}_{i,t} \le P^{BESS-CHmax}_i \tag{47}$$
$$P^{BESS-DImin}_i \le P^{BESS-DI}_{i,t} \le P^{BESS-DImax}_i \tag{48}$$
$$SOC^{min}_i \le SOC_{i,t} \le SOC^{max}_i \tag{49}$$

Equation (50) represents that the state of charge of BESS at the beginning of the dispatch cycle (SOC_{i,t_1}) shall be equal to that at the end of the dispatch cycle ($SOC_{i,t_{24}}$).

$$SOC_{i,t_1} = SOC_{i,t_{24}} \tag{50}$$

6) CAPACITOR BANK

Equation (51) represents the minimum and maximum reactive power limits of capacitor bank on bus i at time t.

$$Q^{CAPmin}_i \le Q^{CAP}_{i,t} \le Q^{CAPmax}_i \tag{51}$$

IV. CASE STUDIES

The effectiveness of the multi-objective optimization is tested on standard IEEE 33-bus radial distribution system. IEEE 33-bus system consists of 32 buses, excluding the main substation bus. The total loads of the system are 3715 kW and 2300 kVAr [35]. The minimum and maximum permissible voltage limits for all buses are considered at ±10%. It is assumed that the current limit of the branches connecting buses 1-10 is 400 A and the remaining branches are rated at 200 A [36].

The proposed model is formulated as a mixed-integer nonlinear programming (MINLP) optimization problem. The model is solved in GAMS [37], [38] environment on Intel (R) Xeon (R) Processor E5-1630 v3 3.70 GHz with 32 GB RAM PC.

Fig. 5 shows the flow chart of the optimization model. The problem is initially solved as a relaxed mixed integer nonlinear programming (RMINLP) optimization problem using MINOS solver, its solution is used as a starting point for the sophisticated MINLP optimization problem which is then solved by BONMIN solver. By providing a good starting point for BONMIN, the chance to obtain a global optimum or even a local optimum that is close to the global optimum is significantly increased and the calculation time is significantly reduced compared to if BONMIN solver is used alone [37].

The simulation time of all the studied cases ranges from 1 second to 624 seconds.

The potential locations for renewable DGs, BESSs, and CBs are assumed to be known as shown in Fig.6 at:

- The far end buses (18, 22, 25, and 33).
- The branching buses (2, 3, and 6).
- The intermediate buses between branching and far end buses (12, 20, and 29).

These locations have been selected after many trials to freely allocate the renewables at all load buses (2 to 33). In these trials, the above-assumed buses were found to be the most frequent buses to host DGs as a result of optimization under the different configurations and cases. Also, the values of the objective functions obtained when freely allocating the DGs on all load buses and those obtained with the controlled allocation of the DGs on the mentioned buses were almost the same. Moreover, allocating DGs on all buses will have practical limitations.

As BESSs and CBs are used in conjunction with intermittent renewable DGs to smooth out their energy delivery and to support their limited reactive power, respectively. Accordingly, the assumption that they have the same potential locations as that of DGs is valid.

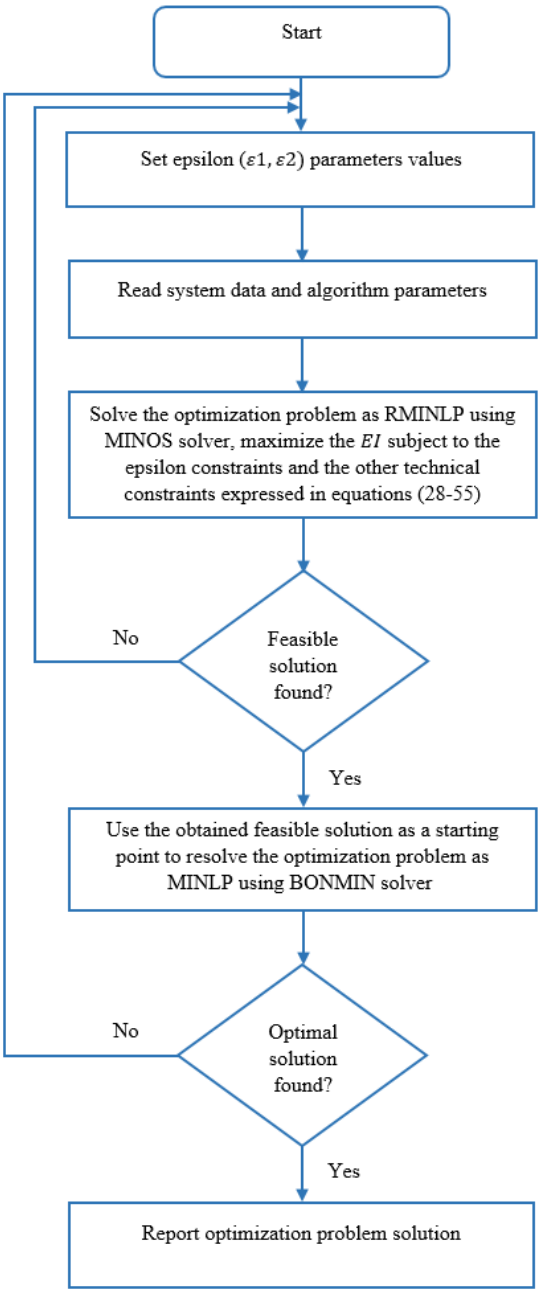

FIGURE 5. Flow chart of the proposed optimization model.

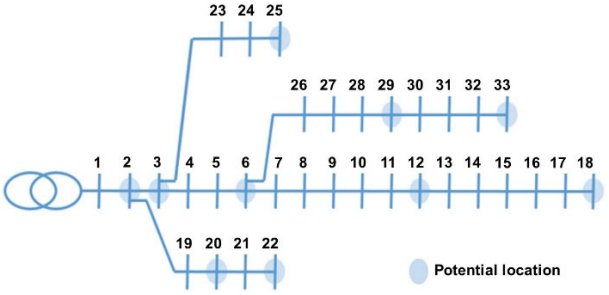

FIGURE 6. Potential locations of renewable DGs, BESSs, and CBs on IEEE 33 bus system.

TABLE 2. The simulation parameters used in the modelling.

Parameter	Value
Installation cost of wind DG (IC^{WDG}) [39]	1473($/kW)
Installation cost of solar DG (IC^{SDG}) [39]	995($/kW)
Installation cost of BESS (IC^{BESS}) [40]	388($/kW) +372($/kWh)
Installation cost of CB (IC^{CB}) [41]	30($/kVAr)
Operation and maintenance cost of wind DG (OMC^{WDG}) (2% of the installation cost/annum)	29.46 ($/kW-year)
Operation and maintenance cost of Solar DG (OMC^{SDG}) (2% of the installation cost/annum)	19.9 ($/kW-year)
Operation and maintenance cost of BESS (OMC^{BESS}) [40]	10 ($/kW-year) +0.0003($/kWh)
Purchased electricity rate (C_{hr}) [42]	0.13 ($/kWh)
DR compensation rate (C_{hr}^{DR})	0.05($/kWh)
Degradation cost of reference BESS per kWh of the discharged energy ($DegC^{BESS-REF}$) [34]	0.042($/kWh)
Installation cost of reference BESS per kWh ($EC^{BESS-REF}$)[34]	312($/kWh)
DR limits at bus i (α_i^{DRmin}, α_i^{DRmax})	20%
Maximum allowable percentage of wind and solar curtailed power (λ_i^{WDG}, λ_i^{SDG})	10 %
Power factor limits of wind and solar DGs ($PF_{i,t}^{WDG}$, $PF_{i,t}^{SDG}$)	0.95 (lead/lag)
Minimum and maximum permissible bus voltage (V_i^{min}, V_i^{max})	0.9,1.1 pu
Minimum and maximum state of charge of BESS at bus i (SOC_i^{min}, SOC_i^{max})	0,300 kWh
Minimum and maximum rating of capacitor bank at bus i (Q_i^{CAPmin}, Q_i^{CAPmax})	0,500 kVAr
BESS charging efficiency ($\eta^{BESS-CH}$)	0.95
BESS discharging efficiency ($\eta^{BESS-DI}$)	0.9
Minimum and maximum limits of BESS charging power at bus i ($P_i^{BESS-CHmin}$, $P_i^{BESS-CHmax}$)	0, 0.2 SOC_i^{max}
Minimum and maximum limits of BESS discharging power at bus i ($P_i^{BESS-DImin}$, $P_i^{BESS-DImax}$)	0, 0.2 SOC_i^{max}
Annual nominal interest rate (IR^*)	2 %
Annual inflation rate (IF)	1%
Life time of wind/solar DG ($N_{y_{WDG}}/N_{y_{SDG}}$)	25 years
Life time of BESS ($N_{y_{BESS}}$)	10 years
Life time of CB ($N_{y_{CB}}$)	10 years

The daily demand load variation on all buses are assumed to be known [38], the daily demand load variations is shown in Fig.7:

The peak demand hours are assumed to be 4 hours from 6 PM to 9 PM. The utility pays incentives to customers who agree to reduce their energy demand during the peak demand hours.

The simulation parameters used in the modelling of the system under study are shown in table 2.

The daily average power losses and voltage stability factor of the studied system under the base case in absence of renewable DGs, DR, BESSs, and CBs are 120.5 kW and 0.958, respectively.

To demonstrate the effectiveness of each of the used tools on the objective functions $OF1$, $OF2$ *and* $OF3$, two different renewable configurations are investigated:

- Configuration 1: Wind DGs.
- Configuration 2: Solar DGs.

In each configuration, five cases are studied:

- Case1: Optimal allocation of DGs.
- Case2: Optimal allocation of DGs in presence of DR.
- Case3: Optimal allocation of DGs in presence of DR and curtailment.
- Case4: Optimal allocation of DGs and BESSs in presence of DR and curtailment.
- Case5: Optimal allocation of DGs, BESSs, and CBs in presence of DR and curtailment.

In each case, several iterations are done. In each iteration, the epsilon parameters $\varepsilon 1$ and/or $\varepsilon 2$ vary, and the multi-objective function is optimized.

The most probable wind and solar power scenarios as generated in Section II are used in the optimization modelling.

The case studies of the two configurations are addressed in the following subsections.

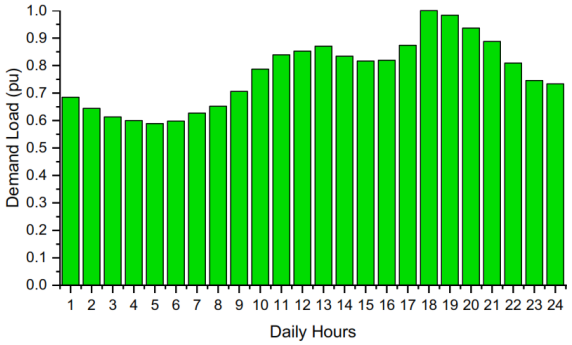

FIGURE 7. Daily demand load variations.

A. CONFIGURATION 1: WIND DGs

In configuration 1, under case 1 and as shown in Fig.8, the highest economic index is 2.54 when the voltage stability factor and power losses are 0.962 and 100 kW, respectively. The economic index reduced slightly with the voltage stability factor increase and the power losses reduction, the highest voltage stability factor and the lowest power losses are 0.975 and 80 kW, respectively.

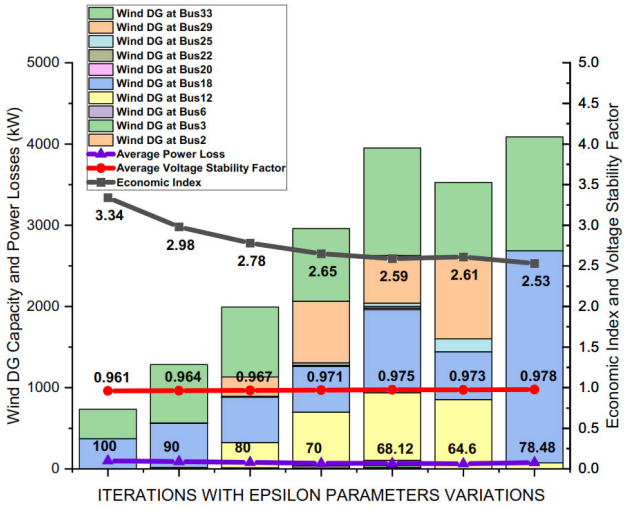

FIGURE 9. Variations of the objective functions and wind DGs capacities with epsilon parameters change under case2.

In presence of DR under case 2 and as shown in Fig.9, the highest economic index is increased by 31.5% as compared to that of case 1. The lowest power losses are reduced by 19.25% and the highest voltage stability factor increased by 0.003 as compared to that of case 1. With the activation of the renewables curtailment option under case 3, it can be seen from Fig.10 that the highest economic index is remained the same as that of case 2. However, the activation of the curtailment option resulted in lower power losses and higher voltage stability factor values compared to case 2. The lowest power losses are reduced by 7.12% and the highest voltage stability factor is increased by 0.003 as compared to that of case 2.

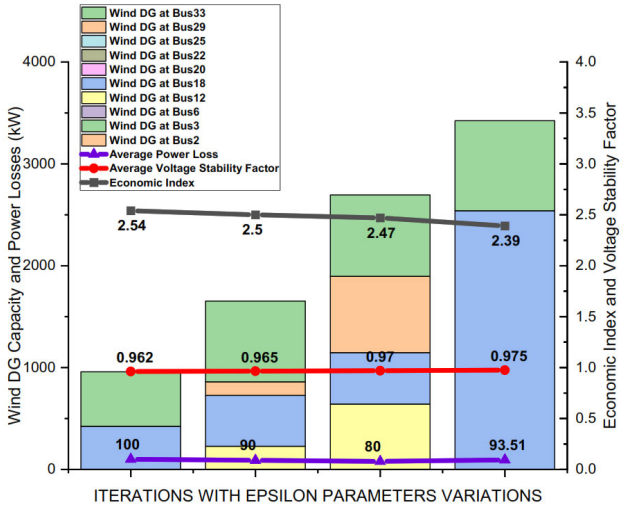

FIGURE 8. Variations of the objective functions and wind DGs capacities with epsilon parameters change under case1.

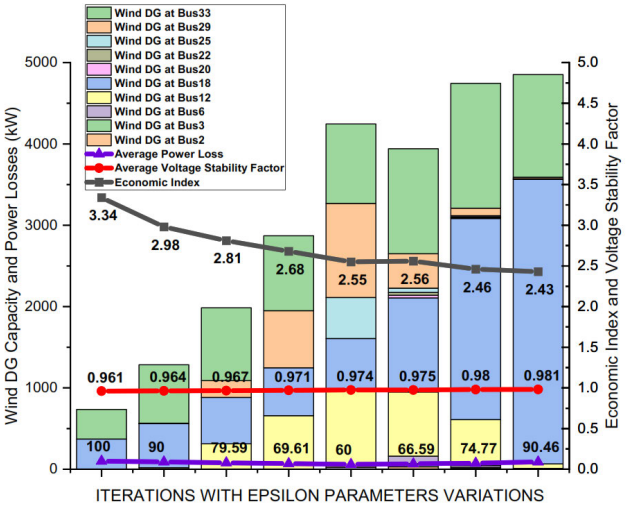

FIGURE 10. Variations of the objective functions and wind DGs capacities with epsilon parameters change under case3.

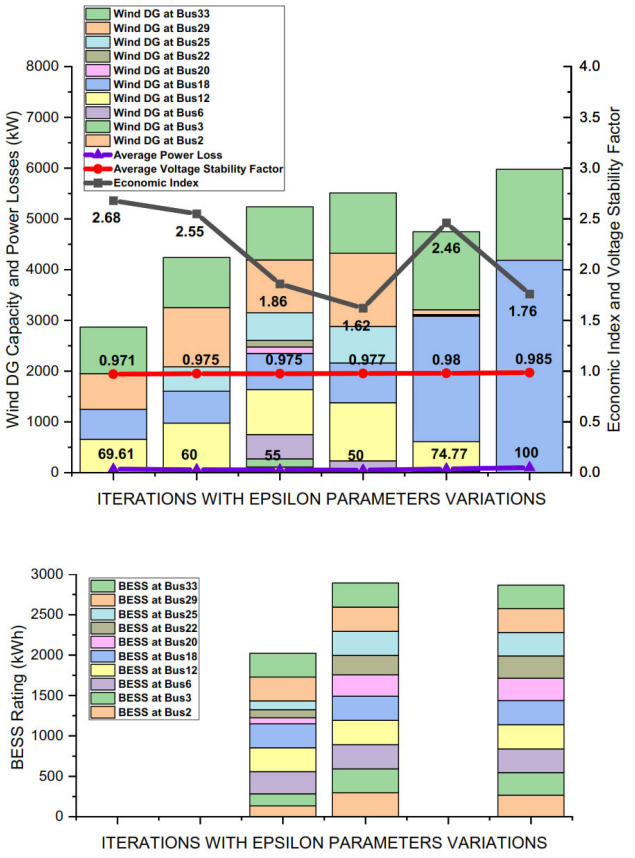

FIGURE 11. (a)Variations of the objective functions and wind DGs capacities with epsilon parameters change under case4. (b) Variations of BESSs ratings under case4.

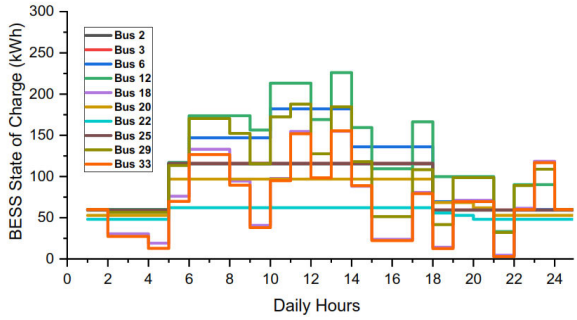

FIGURE 12. State of charge of the BESS under the lowest power losses iteration of case 4.

By utilizing the BESSs side by side with DR and curtailment under case 4 and as shown in Fig.11 (a), it can be seen that the highest voltage stability factor is increased by 0.010, 0.007, and 0.004 as compared to cases 1, 2, and 3, respectively. It can be also seen that the lowest power losses under case 4 are reduced by 37.5%, 22.6%, and 16.66% as compared to cases 1, 2, and 3, respectively. The ratings of the required BESSs at the different buses under case 4 are shown in Fig.11 (b), the total BESSs rating required to achieve the highest voltage stability factor of 0.985 is almost the same as that required to achieve the lowest power losses of 50 kW.

The state of charge variations of the BESSs during the 24 hours under the lowest power losses iteration of case 4 are shown in Fig. 12.

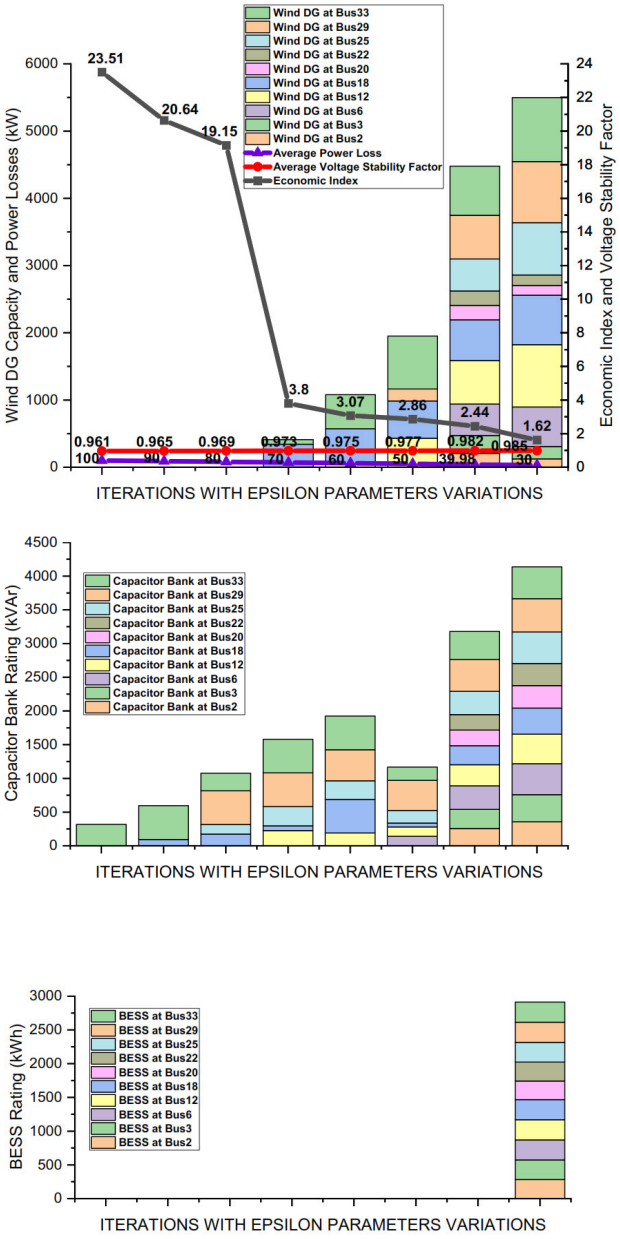

FIGURE 13. (a) Variations of the objective functions and wind DGs capacities with epsilon parameters change under case5. (b) Variations of CBs ratings under case5. (c) Variations of BESSs ratings under case5.

In case 5, the CBs are integrated with BESSs, DR, and curtailment. The shown results in Fig.13 (a) reveal that the highest economic index among the 5 studied cases is obtained at 23.51. It can be seen that this value is achieved in absence of BESSs and with no wind DG installed at any bus. This high economic index value represents the economic benefits that could be obtained with the integration of CBs. The lowest power losses and the highest voltage stability factor values among the 5 studied cases are achieved under case 5. The

lowest power losses are reduced by 62.5%, 53.56%, 50%, and 40% as compared to cases 1, 2, 3, and 4, respectively. The highest voltage stability factor is the same as that of case 4.

The ratings of the required CBs at the different buses are shown in Fig.13 (b). The total rating of the CBs to achieve the highest economic index is the lowest among all iterations under case 5. Fig.13(c) shows that no BESSs are required in all iterations unless to achieve lower power losses of 30 kW.

The state of charge variations of the BESSs during the 24 hours under the lowest power losses iteration of case 5 are shown in Fig. 14.

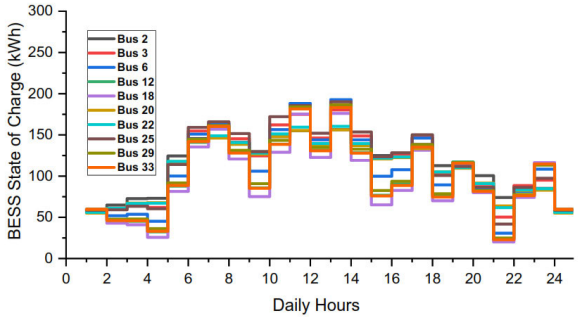

FIGURE 14. State of charge of the BESSs under the lowest power losses iteration of case 5.

The variations of the injected reactive power by the CBs during the 24 hours of case 5 under the lowest power losses iteration are shown in Fig. 15.

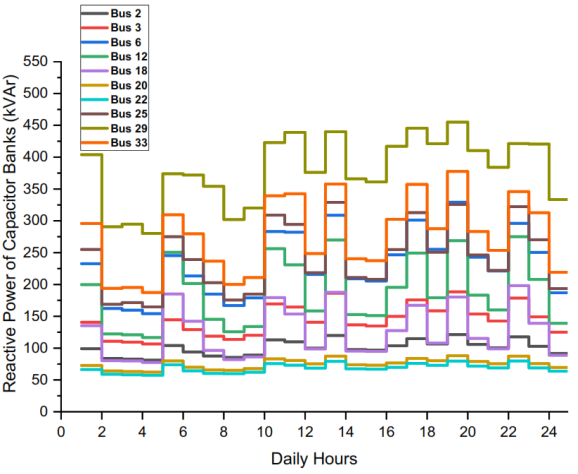

FIGURE 15. Reactive power of the CBs under the lowest power losses iteration of case 5.

Fig.16 shows the mean bus voltage profile considering the lowest power losses iterations for the 5 studied cases under configuration 1. With the BESSs integration under case 4, the voltage profile is enhanced compared to cases 1, 2, and 3. It is also clear that the CBs integration under case 5 has substantially improved the voltage profile compared to all the other cases.

The most optimal results for the three main objectives of all the studied cases under configuration 1 are presented in bold in table 3.

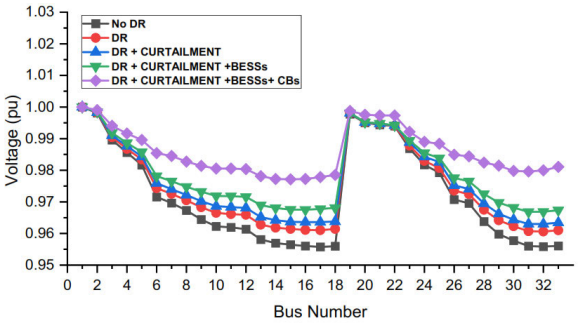

FIGURE 16. Mean bus voltage profile for the lowest power losses iterations of the 5 studied cases under configuration 1.

TABLE 3. The most optimal results of the main objectives for the 5 studied cases under configuration 1.

Studied Case	EI	P_{LOSS}^{AV}(kW)	VSF^{AV}
Case 1	**2.54**	100	0.962
	2.47	**80**	0.970
	2.39	93.51	**0.975**
Case 2	**3.34**	100	0.961
	2.61	**64.6**	0.973
	2.53	78.48	**0.978**
Case 3	**3.34**	100	0.961
	2.55	**60**	0.974
	2.43	90.46	**0.981**
Case 4	**2.68**	69.61	0.971
	1.62	**50**	0.977
	1.76	100	**0.985**
Case 5	**23.51**	100	0.961
	1.62	**30**	**0.985**

B. CONFIGURATION 2: SOLAR DGs

In configuration 2, under case 1 and as shown in Fig.17, the highest economic index is 7.09 when the voltage stability

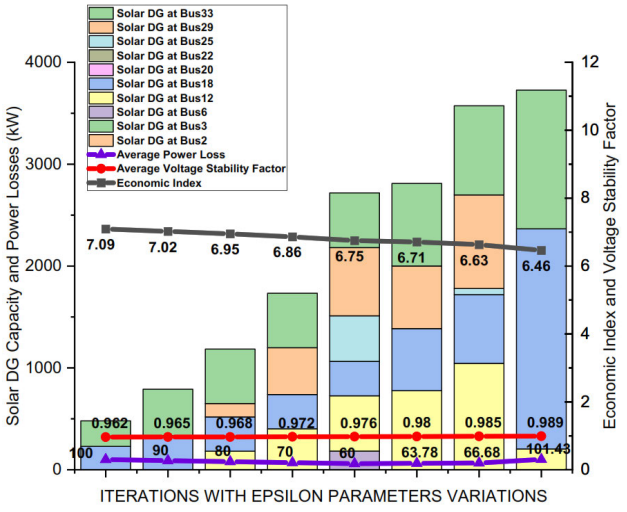

FIGURE 17. Variations of the objective functions and solar DGs capacities with epsilon parameters change under case1.

factor and power losses are 0.962 and 100 kW, respectively. The economic index is reduced with the voltage stability factor increase and power losses reduction, the highest voltage stability factor and the lowest power losses are 0.989 and 60 kW, respectively. With the integration of DR under case 2, it can be seen from Fig. 18 that the highest economic index is 10.46, improved by 47.53% as compared to that of case 1. The lowest power losses are reduced by 33.42% and the highest voltage stability factor is increased by 0.006 as compared to that of case 1.

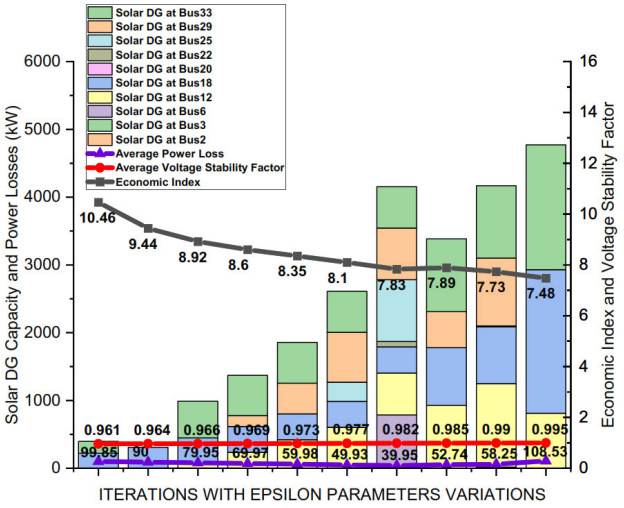

FIGURE 18. Variations of the objective functions and solar DGs capacities with epsilon parameters change under case2.

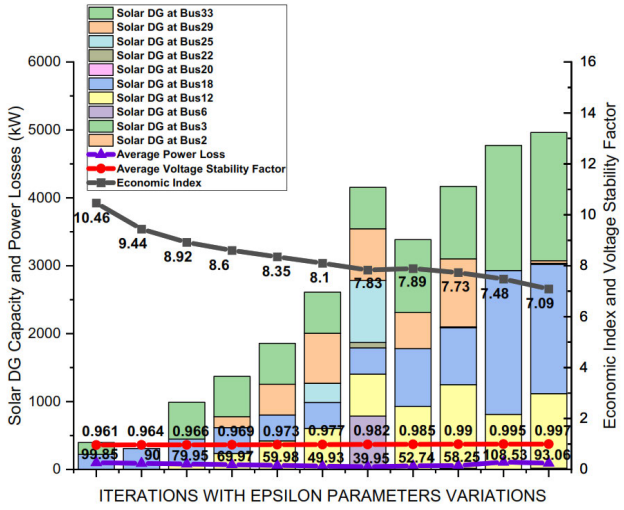

FIGURE 19. Variations of the objective functions and solar DGs capacities with epsilon parameters change under case3.

In case 3, the renewables curtailment option is activated along with DR. Fig. 19 shows that the obtained results are the same as that of case 2 including the highest economic index and the lowest power losses values, however the highest voltage stability factor is increased by 0.002 as compared to that of case 2. This indicates that curtailment could be an effective option in some cases.

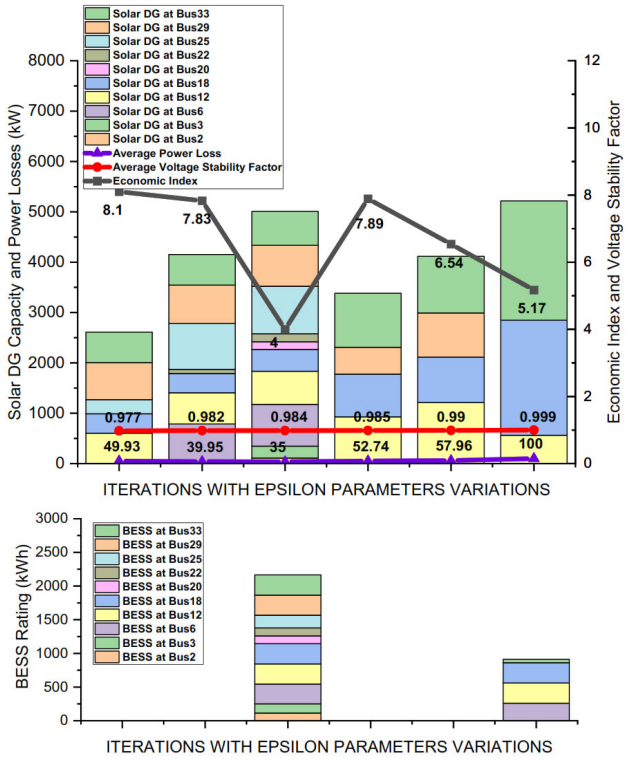

FIGURE 20. (a)Variations of the objective functions and solar DGs capacities with epsilon parameters change under case4. (b) Variations of BESSs ratings under case4.

The BESSs are integrated with DR and curtailment under case 4. From Fig.20 (a), the lowest power losses are reduced by 41.67% as compared to case 1 and reduced by 12.39% as compared to cases 2 and 3. The highest voltage stability factor is increased by 0.01, 0.004, and 0.002 as compared to cases 1, 2, and 3, respectively. The ratings of the required BESSs at the different buses are shown in Fig.20 (b), a higher total BESSs rating is required to achieve the lowest power losses of 35 kW than the total BESSs rating required to achieve the highest voltage stability factor of 0.999.

The state of charge variations of the BESSs during the 24 hours under the lowest power losses iteration of case 4 are shown in Fig. 21.

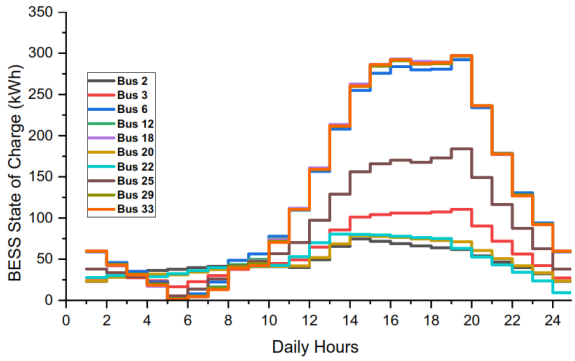

FIGURE 21. State of charge of the BESSs under the lowest power losses iteration of case 4.

With the integration of CBs, BESSs, DR, and curtailment under case 5. The results presented in Fig.22 (a) show that the highest economic index is 23.51 (same as that obtained in configuration 1 under case 5) which is the highest among the 5 studied cases. This value is achieved in absence of BESSs and with no solar DG installed at any bus. The lowest power losses and the highest voltage stability factor values among the 5 cases are also achieved under case 5. The lowest power losses are reduced by 66.7% compared to case1, reduced by 49.99% as compared to cases 2 and 3, and reduced by 42.91% as compared to case 4. The highest voltage stability factor is the same as that of case 4.

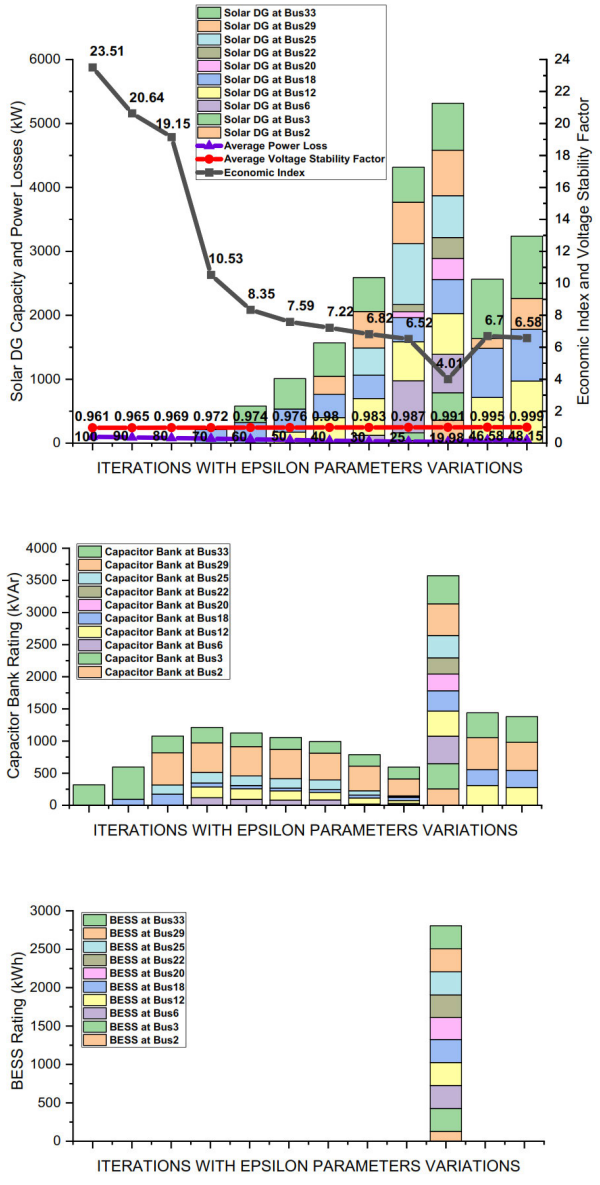

FIGURE 22. (a) Variations of the objective functions and solar DGs capacities with epsilon parameters change under case5. (b) Variations of CBs ratings under case5. (c) Variations of BESSs ratings under case5.

The ratings of the required CBs at the different buses are shown in Fig.22 (b).

Fig.22(c) shows that no BESSs are required in all iterations unless to achieve lower power losses of 19.98 kW.

The state of charge variations of the BESSs during the 24 hours under the lowest power losses iteration of case 5 are shown in Fig. 23.

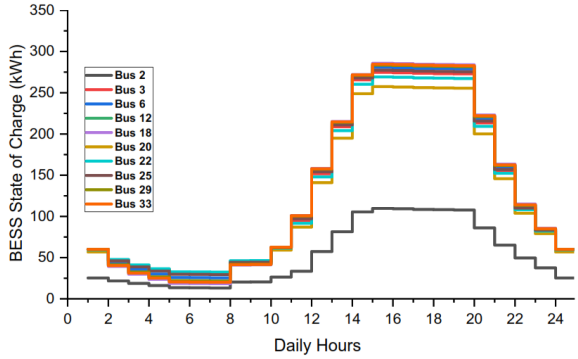

FIGURE 23. State of charge of the BESSs under the lowest power losses iteration of case 5.

The variations of the injected reactive power by the CBs during the 24 hours under the lowest power losses iteration of case 5 are shown in Fig. 24.

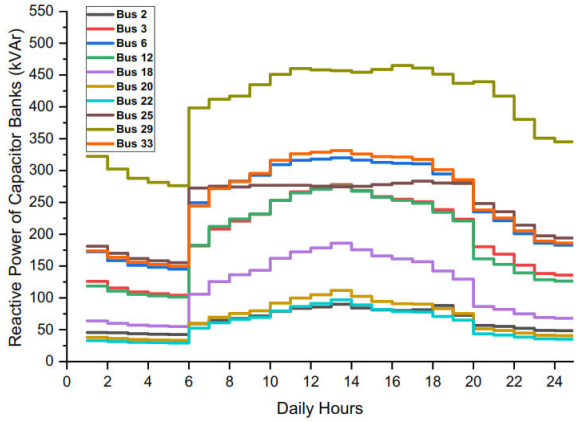

FIGURE 24. Reactive power of the capacitor banks under the lowest power losses iteration of case 5.

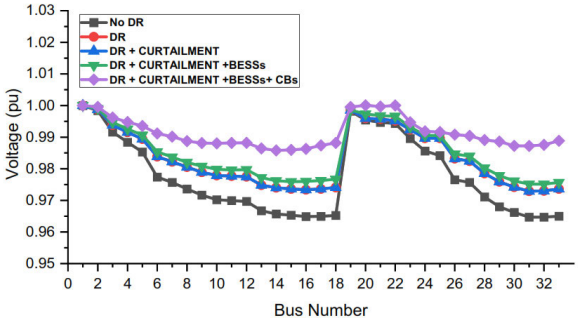

FIGURE 25. Mean bus voltage profile for the lowest power losses iterations of the 5 studied cases under configuration 2.

Fig.25 shows the mean bus voltage profile considering the lowest power losses iterations for the 5 studied cases under configuration 2. With the integration of BESSs under case 4,

the voltage profile is enhanced compared to cases 1, 2, and 3. It is also clear that the CBs integration under case 5 has substantially improved the voltage profile compared to all the other cases.

The most optimal results for the three main objectives of all the studied cases under configuration 2 are presented in bold in table 4.

TABLE 4. The most optimal results of the main objectives for the 5 studied cases under configuration 2.

Studied Case	EI	P_{LOSS}^{AV}(kW)	VSF^{AV}
Case 1	**7.09**	100	0.962
	6.75	**60**	0.976
	6.46	101.43	**0.989**
Case 2	**10.46**	99.85	0.961
	7.83	**39.95**	0.982
	7.48	108.53	**0.995**
Case 3	**10.46**	99.85	0.961
	7.83	**39.95**	0.982
	7.09	93.06	**0.997**
Case 4	**8.1**	49.93	0.977
	4	**35**	0.984
	5.17	100	**0.999**
Case 5	**23.51**	100	0.961
	4.01	**19.98**	0.991
	6.58	48.15	**0.999**

C. ANALYSIS OF THE OBTAINED RESULTS

In this study, the economic feasibility is analyzed by the obtained economic index values, while the technical feasibility is analyzed through the obtained power losses and voltage stability factor values. Based on the obtained results, the economic and technical feasibility of the used tools has been proven under both wind and solar configurations. In case 1 of the two configurations, lower power losses and higher voltage stability factor values are obtained compared to the base case in which no renewable DGs are integrated while the economic index is kept at reasonable values. In case 2, the DR integration with renewables resulted in better voltage stability factor and power losses values compared to case 1, also the economic index increased significantly with DR integration because of the DR compensation paid to customers. In case 3, the curtailment integration slightly enhanced the voltage stability factor and power losses values, but no sensible impact on the economic index values is recorded. This is understandable as the curtailment option has no direct relation to the economic index cost terms. In case 4, the BESS integration resulted in much lower power losses and higher voltage stability factor values.

However, the economic index is reduced in the iterations where BESSs are utilized because of the relatively high installation and degradation costs of the BESSs. The CBs integration in case 5 resulted in the highest economic index and voltage stability factor values, and the lowest power losses among all the studied cases. This could be interpreted because of the relatively low installation cost of the CBs which improves the economic index, also the reactive power compensation provided by the CBs reduces the power losses and improves the voltage stability factor.

It is observed that the resulted economic index values in configuration 2 using solar DGs are higher than that of configuration 1 using wind DGs under the same cases. This is because of the higher installation, operation and maintenance costs of the wind DGs compared to that of solar DGs for the same power. Also, the wind speed, solar irradiance, and their associated generated power pattern greatly affect the economic feasibility, such that the higher wind speed and solar irradiance, the better utilization of the peak installed wind and solar power and accordingly the better economic feasibility. Furthermore, the mismatching between the daily demand loads and renewable generation patterns such that maximum power generation and minimum load consumption and vice versa greatly affect the economics of renewables integration.

Among the tools used in the optimization model, the CBs demonstrated the highest economic feasibility while the BESSs are of the lowest economic feasibility. This is mainly because of the relatively low installation cost of the CBs and the relatively high installation and degradation costs of the BESSs. However, the integration of BESSs is still required under some cases to overcome the mismatching between renewables' power generation and load, and to achieve lower power losses and higher voltage stability factors that are not achievable without BESSs.

V. CONCLUSION

In this paper, a multi-objective optimization problem is formulated to maximize the economic index and average voltage stability factor, and to minimize the average power losses in distribution networks considering the simultaneous integration of different renewable DGs, BESSs, and CBs in presence of DR and renewables curtailment, and considering the battery degradation cost. The modelling of wind and solar generated power is considered. The proposed model is implemented and tested on standard IEEE 33-bus radial distribution system.

Two different configurations are investigated using wind and solar DGs, in each configuration five different cases are studied. Several iterations are done under each case in which the epsilon parameters vary and the multi-objective function is optimized. The key findings of the study are addressed in the following points:

- The renewable DGs integration in the distribution network in case 1 has technical and economic benefits. The technical benefits are assured by achieving lower power losses and higher voltage stability factor values compared to the base case without renewable DGs, while the economic feasibility is guaranteed by achieving reasonable economic index values.

- The DR has a positive effect in optimizing the multi-objectives. The economic index is increased significantly with DR integration in case 2 because of the compensation paid to customers for energy consumption reduction during the peak demand hours. The highest economic index is increased by 31.5% and 47.53% for wind and solar configurations, respectively with the activation of DR compared to that without DR. Also, the power losses are reduced and the voltage stability factor is improved with DR integration.
- The integration of renewables curtailment in case 3 has no sensible impact on the economic index values, however it is useful in achieving lower power losses and higher voltage stability factor values.
- The BESSs demonstrated to have the lowest economic feasibility among the used tools in the modelling. The economic index is reduced significantly with the integration of BESSs because of the additional costs of the BESSs. However, the integration of BESSs is still required under some iterations under case 4 to meet certain objectives such as lower power losses (50 kW and 35 kW for wind and solar configurations, respectively) and/or higher voltage stability factor (0.985 and 0.999 for wind and solar configurations, respectively).
- The CBs demonstrated to have the highest economic feasibility among the used tools in the modelling. The highest economic index is achieved under case 5 of wind and solar configurations at 23.51. This value is achieved in conjunction with DR and curtailment and in absence of wind and solar DGs, and BESSs.
- The simultaneous integration of renewable DGs, BESSs, and CBs in presence of DR and renewables curtailment under case 5 achieved the lowest power losses (30 kW and 19.98 kW for wind and solar configurations, respectively) and the highest voltage stability factor (0.985 and 0.999 for wind and solar configurations, respectively) among all cases.
- The economic index values obtained for solar configuration are higher than that of the wind configuration under the same cases due to the high installation, operation and maintenance costs of wind DGs as compared to that of solar DGs.
- The mean voltage profile improved under wind and solar configurations with the integration of each of the used tools. The substantial improvement of voltage profile is achieved by BESSs and CBs integration.

REFERENCES

[1] International Renewable Energy Agency, Abu Dhabi, United Arab Emirates. (Apr. 2020). *Global Renewables Outlook: Energy Transformation 2050 (Edition: 2020)*. [Online]. Available: https://www.irena.org/publications/2020/Apr/Global-Renewables-Outlook-2020

[2] G. S. Chawda and A. G. Shaik, "Enhancement of wind energy penetration levels in rural grid using ADALINE-LMS controlled distribution static compensator," *IEEE Trans. Sustain. Energy*, vol. 13, no. 1, pp. 135–145, Jan. 2022, doi: 10.1109/TSTE.2021.3105423.

[3] P. S. Georgilakis and N. D. Hatziargyriou, "Optimal distributed generation placement in power distribution networks: Models, methods, and future research," *IEEE Trans. Power Syst.*, vol. 28, no. 3, pp. 3420–3428, Aug. 2013, doi: 10.1109/TPWRS.2012.2237043.

[4] A. Keane, L. F. Ochoa, C. L. T. Borges, G. W. Ault, A. D. Alarcon-Rodriguez, R. A. F. Currie, F. Pilo, C. Dent, and G. P. Harrison, "State-of-the-art techniques and challenges ahead for distributed generation planning and optimization," *IEEE Trans. Power Syst.*, vol. 28, no. 2, pp. 1493–1502, May 2013, doi: 10.1109/TPWRS.2012.2214406.

[5] P. H. A. Mahmoud, P. D. Huy, and V. K. Ramachandaramurthy, "A review of the optimal allocation of distributed generation: Objectives, constraints, methods, and algorithms," *Renew. Sustain. Energy Rev.*, vol. 75, pp. 293–312, Aug. 2017, doi: 10.1016/j.rser.2016.10.071.

[6] S. S. Kola, "A review on optimal allocation and sizing techniques for DG in distribution systems," *Int. J. Renew. Energy Res.*, vol. 8, no. 3, pp. 1236–1256, 2018.

[7] M. Duong, T. Pham, T. Nguyen, A. Doan, and H. Tran, "Determination of optimal location and sizing of solar photovoltaic distribution generation units in radial distribution systems," *Energies*, vol. 12, no. 1, p. 174, Jan. 2019, doi: 10.3390/en12010174.

[8] A. Ahmed, M. F. Nadeem, I. A. Sajjad, R. Bo, I. A. Khan, and A. Raza, "Probabilistic generation model for optimal allocation of wind DG in distribution systems with time varying load models," *Sustain. Energy, Grids Netw.*, vol. 22, Jun. 2020, Art. no. 100358, doi: 10.1016/j.segan.2020.100358.

[9] R. Fathi, B. Tousi, and S. Galvani, "A new approach for optimal allocation of photovoltaic and wind clean energy resources in distribution networks with reconfiguration considering uncertainty based on info-gap decision theory with risk aversion strategy," *J. Cleaner Prod.*, vol. 295, May 2021, Art. no. 125984, doi: 10.1016/j.jclepro.2021.125984.

[10] A. S. Hassan, Y. Sun, and Z. Wang, "Multi-objective for optimal placement and sizing DG units in reducing loss of power and enhancing voltage profile using BPSO-SLFA," *Energy Rep.*, vol. 6, pp. 1581–1589, Nov. 2020, doi: 10.1016/j.egyr.2020.06.013.

[11] Z. Li, S. Wang, Y. Zhou, W. Liu, and X. Zheng, "Optimal distribution systems operation in the presence of wind power by coordinating network reconfiguration and demand response," *Int. J. Electr. Power Energy Syst.*, vol. 119, Jul. 2020, Art. no. 105911, doi: 10.1016/j.ijepes.2020.105911.

[12] M. McPherson and B. Stoll, "Demand response for variable renewable energy integration: A proposed approach and its impacts," *Energy*, vol. 197, Apr. 2020, Art. no. 117205, doi: 10.1016/j.energy.2020.117205.

[13] E. Sarker, M. Seyedmahmoudian, E. Jamei, B. Horan, and A. Stojcevski, "Optimal management of home loads with renewable energy integration and demand response strategy," *Energy*, vol. 210, Nov. 2020, Art. no. 118602, doi: 10.1016/j.energy.2020.118602.

[14] S. M. Hakimi, A. Hasankhani, M. Shafie-Khah, and J. P. S. Catalão, "Optimal sizing and siting of smart microgrid components under high renewables penetration considering demand response," *IET Renew. Power Gener.*, vol. 13, no. 10, pp. 1809–1822, Jul. 2019, doi: 10.1049/iet-rpg.2018.6015.

[15] M. Alilou, D. Nazarpour, and H. Shayeghi, "Multi-objective optimization of demand side management and multi DG in the distribution system with demand response," *J. Oper. Autom. Power Eng.*, vol. 6, no. 2, pp. 230–242, 2018, doi: 10.22098/joape.2006.4207.1328.

[16] A. H. Taha, H. M. Alham, and K. M. H. Youssef, "Hosting capacity maximization of wind and solar DGs in distribution networks using demand response and renewables curtailment," *Int. J. Energy Convers.*, vol. 9, no. 3, pp. 103–112, May 2021, doi: 10.15866/irecon.v9i3.20066.

[17] N. Etherden and M. H. J. Bollen, "Increasing the hosting capacity of distribution networks by curtailment of renewable energy resources," in *Proc. IEEE Trondheim PowerTech*, Jun. 2011, pp. 1–7, doi: 10.1109/PTC.2011.6019292.

[18] A. Karimi, F. Aminifar, A. Fereidunian, and H. Lesani, "Energy storage allocation in wind integrated distribution networks: An MILP-based approach," *Renew. Energy*, vol. 134, pp. 1042–1055, Apr. 2019, doi: 10.1016/j.renene.2018.11.034.

[19] C. Liang, P. Wang, X. Han, W. Qin, Y. Jia, and T. Yuan, "Battery energy storage selection based on a novel intermittent wind speed model for improving power system dynamic reliability," *IEEE Trans. Smart Grid*, vol. 9, no. 6, pp. 6084–6094, Nov. 2018, doi: 10.1109/TSG.2017.2703578.

[20] S. Zhong, J. Qiu, L. Sun, Y. Liu, C. Zhang, and G. Wang, "Coordinated planning of distributed WT, shared BESS and individual VESS using a two-stage approach," *Int. J. Electr. Power Energy Syst.*, vol. 114, Jan. 2020, Art. no. 105380, doi: 10.1016/j.ijepes.2019.105380.

[21] M. Ahmadi, M. E. Lotfy, A. M. Howlader, A. Yona, and T. Senjyu, "Centralised multi-objective integration of wind farm and battery energy storage system in real-distribution network considering environmental, technical and economic perspective," *IET Gener., Transmiss. Distrib.*, vol. 13, no. 22, pp. 5207–5217, Nov. 2019, doi: 10.1049/iet-gtd.2018.6749.

[22] A. Valencia, R. A. Hincapie, and R. A. Gallego, "Optimal location, selection, and operation of battery energy storage systems and renewable distributed generation in medium–low voltage distribution networks," *J. Energy Storage*, vol. 34, Feb. 2021, Art. no. 102158, doi: 10.1016/j.est.2020.102158.

[23] M. Ahmadi, O. B. Adewuyi, M. S. S. Danish, P. Mandal, A. Yona, and T. Senjyu, "Optimum coordination of centralized and distributed renewable power generation incorporating battery storage system into the electric distribution network," *Int. J. Electr. Power Energy Syst.*, vol. 125, Feb. 2021, Art. no. 106458, doi: 10.1016/j.ijepes.2020.106458.

[24] P. Kayal and C. K. Chanda, "Strategic approach for reinforcement of intermittent renewable energy sources and capacitor bank for sustainable electric power distribution system," *Int. J. Electr. Power Energy Syst.*, vol. 83, pp. 335–351, Dec. 2016, doi: 10.1016/j.ijepes.2016.04.029.

[25] S. Zeynali, N. Rostami, and M. R. Feyzi, "Multi-objective optimal short-term planning of renewable distributed generations and capacitor banks in power system considering different uncertainties including plug-in electric vehicles," *Int. J. Electr. Power Energy Syst.*, vol. 119, Jul. 2020, Art. no. 105885, doi: 10.1016/j.ijepes.2020.105885.

[26] A. A. A. El-Ela, R. A. El-Sehiemy, and A. S. Abbas, "Optimal placement and sizing of distributed generation and capacitor banks in distribution systems using water cycle algorithm," *IEEE Syst. J.*, vol. 12, no. 4, pp. 3629–3636, Dec. 2018, doi: 10.1109/JSYST.2018.2796847.

[27] M. Z. Malik, M. Kumar, A. M. Soomro, M. H. Baloch, M. Farhan, M. Gul, and G. S. Kaloi, "Strategic planning of renewable distributed generation in radial distribution system using advanced MOPSO method," *Energy Rep.*, vol. 6, pp. 2872–2886, Nov. 2020, doi: 10.1016/j.egyr.2020.10.002.

[28] M. Aryanezhad, "Management and coordination of LTC, SVR, shunt capacitor and energy storage with high PV penetration in power distribution system for voltage regulation and power loss minimization," *Int. J. Elect. Power Energy Syst.*, vol. 100, pp. 178–192, Sep. 2018, doi: 10.1016/j.ijepes.2018.02.015.

[29] S. Sharma, K. R. Niazi, K. Verma, and T. Rawat, "Coordination of different DGs, BESS and demand response for multi-objective optimization of distribution network with special reference to Indian power sector," *Int. J. Electr. Power Energy Syst.*, vol. 121, Oct. 2020, Art. no. 106074, doi: 10.1016/j.ijepes.2020.106074.

[30] M. Ahmadi, M. E. Lotfy, M. S. S. Danish, S. Ryuto, A. Yona, and T. Senjyu, "Optimal multi-configuration and allocation of SVR, capacitor, centralised wind farm, and energy storage system: A multi-objective approach in a real distribution network," *IET Renew. Power Gener.*, vol. 13, no. 5, pp. 762–773, 2019, doi: 10.1049/iet-rpg.2018.5057.

[31] M. S. Rawat and S. Vadhera, "Maximum penetration level evaluation of hybrid renewable DGs of radial distribution networks considering voltage stability," *J. Control, Autom. Electr. Syst.*, vol. 30, no. 5, pp. 780–793, Oct. 2019, doi: 10.1007/s40313-019-00477-8.

[32] A. T. Al-Awami, M. W. Khalid, and M. A. El-Sharkawi, "An efficient scenario generation technique for short-term wind power production," in *Proc. IEEE Int. Conf. Probabilistic Methods Appl. to Power Syst. (PMAPS)*, Jun. 2018, pp. 1–6, doi: 10.1109/PMAPS.2018.8440538.

[33] A. Gailani, M. Al-Greer, M. Short, and T. Crosbie, "Degradation cost analysis of Li-ion batteries in the capacity market with different degradation models," *Electronics*, vol. 9, no. 1, p. 90, Jan. 2020, doi: 10.3390/electronics9010090.

[34] A. Muqbel, A. T. Al-Awami, and M. Parvania, "Optimal planning of distributed battery energy storage systems in unbalanced distribution networks," *IEEE Syst. J.*, early access, Sep. 1, 2021, doi: 10.1109/JSYST.2021.3099439.

[35] V. Vita, "Development of a decision-making algorithm for the optimum size and placement of distributed generation units in distribution networks," *Energies*, vol. 10, no. 9, p. 1433, Sep. 2017, doi: 10.3390/en10091433.

[36] M. R. M. Cruz, D. Z. Fitiwi, S. F. Santos, and J. P. S. Catalao, "Influence of distributed storage systems and network switching/reinforcement on RES-based DG integration level," in *Proc. 13th Int. Conf. Eur. Energy Market (EEM)*, Jun. 2016, pp. 1–5, doi: 10.1109/EEM.2016.7521337.

[37] *GAMS Documentation*, GAMS Develop. Corp., Fairfax, VA, USA, Apr. 2021.

[38] A. Soroudi, *Power System Optimization Modeling in GAMS*. Cham, Switzerland: Springer, 2017, doi: 10.1007/978-3-319-62350-4.

[39] International Renewable Energy Agency, Abu Dhabi, United Arab Emirates. (Jun. 2020). *Renewable Power Generation Costs in 2019*. [Online]. Available: https://www.irena.org/publications/2020/Jun/Renewable-Power-Costs-in-2019.

[40] K. Mongird, V. Viswanathan, P. Balducci, J. Alam, V. Fotedar, V. Koritarov, and B. Hadjerioua, "Energy storage technology and cost characterization report," Pacific Northwest Nat. Lab., Richland, WA, USA, Tech. Rep. PNNL-28866, Jul. 2019. [Online]. Available: https://energystorage.pnnl.gov/pdf/PNNL-28866.pdf

[41] V. Tamilselvan, T. Jayabarathi, T. Raghunathan, and X.-S. Yang, "Optimal capacitor placement in radial distribution systems using flower pollination algorithm," *Alexandria Eng. J.*, vol. 57, no. 4, pp. 2775–2786, Dec. 2018, doi: 10.1016/j.aej.2018.01.004.

[42] Gas, Coal and Power Markets (GCP) Division of the International Energy Agency (IEA). (Dec. 2020). *Electricity Market Report*. [Online]. Available: https://www.iea.org/reports/electricity-market-report-december-2020

HAITHAM A. TAHA was born in Egypt, in October 1984. He received the B.Sc. and M.Sc. degrees in electrical power engineering from Cairo University, Giza, Egypt, in 2006 and 2010, respectively, where he is currently pursuing the Ph.D. degree in electrical engineering with the Faculty of Engineering. He is currently working as a Senior Electrical Design Engineer with Dar Al-Handasah Consultants (Shair and Partners). His research interests include wind and solar renewable energy sources, mathematical optimization, power system planning, and optimum power flow.

M. H. ALHAM was born in Egypt, in May 1985. He received the B.Sc., M.Sc., and Ph.D. degrees in electric power engineering from Cairo University, in 2007, 2012, and 2016, respectively. Since August 2016, he has been an Assistant Professor with Cairo University. His research interests include power system economic operation, distributed generation, and renewable energy sources.

HOSAM K. M. YOUSSEF was born in Cairo, Egypt, in August 1956. He received the B.Sc. degree in electronics engineering and the M.Sc. degree in power and machines engineering from Cairo University, Egypt, in 1979 and 1982, respectively, and the Ph.D. degree from the University of Windsor, Canada, in 1988. He was appointed as an Assistant Professor with the Faculty of Engineering, Cairo University, in 1988. He was on leave of absence from Cairo University, from 1992 to 2001, where he was an Assistant Professor and then an Associate Professor with the Public Authority, Applied Education and Training, Kuwait. He has been a Professor with the Electrical Engineering Department, Faculty of Engineering, Cairo University, since 2002. His research interests include power system planning, power quality, renewable energy sources, and optimization.